Chiral quark soliton model and flavor-asymmetric $q\bar{q}$ sea in the nucleon

M. Wakamatsu
Department of Physics, Faculty of Science, Osaka University, Toyonaka, Osaka 560, Japan
(Received 26 May 1992)

By making full use of the advantage of the chiral quark soliton model, we investigate the flavor structure of the sea-quark components in the nucleon. First, through the analysis of the charge distributions of the proton and neutron, we demonstrate that the effect of sea quarks incorporated in this model can be identified with that of the cloud of pions surrounding the core of three valence quarks. Next, not only the integrated value but also the spatial structure of the $q\bar{q}$ scalar condensate in the nucleon is studied with emphasis upon the separate functions of the valence and sea quarks. The enhancement of the $\bar{d}d$ scalar condensate relative to the $\bar{u}u$ one in the proton is shown to be consistent with QCD phenomenology. We have also carried out a theoretical analysis of the Gottfried sum on the basis of the chiral quark soliton model and obtained a satisfactory agreement with the recent New Muon Collaboration measurement.

PACS number(s): 13.60.Hb, 11.30.Rd, 12.40.Aa, 13.40.Fn

I. INTRODUCTION

In constructing a low-energy effective theory of QCD, an important question is which aspects of QCD should be taken in among others. Quark confinement would certainly be a fundamental nature of the QCD Lagrangian, but in most cases low-energy properties of hadrons are rather insensitive to the mechanism of confinement, once the hadronic wave functions with damping tail can be successfully constructed. On the contrary, the long history of hadron physics tells us that no theory of hadrons could be realistic without taking account of the spontaneous chiral-symmetry breaking of the QCD vacuum. The nonvanishing quark condensate and the appearance of the Nambu-Goldstone pions are characteristic features of this chiral-asymmetric vacuum. The appearance of this nearly massless excitation is naturally expected to have significant effects also on the properties of baryons. Shuryak even emphasized that spontaneous chiral-symmetry breaking determines not only the long-range part of hadronic physics (the one-pion-exchange forces, etc.) but also turns out to be the key ingredient for understanding the opposite limit, providing the main nonperturbative corrections to the correlation functions in the QCD vacuum at small distances [1].

Some years ago, Diakonov and co-workers proposed a model of the nucleon based on an extremely simple effective chiral action which incorporates the above features of low-energy QCD [2,3]. This effective action contains only two residual effective degrees of freedom parametrizing the low-energy QCD: i.e., the Nambu-Goldstone pion and the quarks. (The gluon fields are integrated out to obtain this effective action, and in this sense they are contained in it as implicit degrees of freedom.) The pion field, which is treated at the classical level, plays the role of the Hartree-type mean field for quarks to form a solitonlike bound state [3–10]. The nontrivial topology of this Hartree potential makes the above bound state closely resemble a Skyrmion, although one should not also forget about crucial differences between them [10,11].

From a practical viewpoint, the greatest advantage of the chiral quark soliton model is that it enables us to solve the nucleon bound-state problem with full inclusion of the Dirac-sea-quark degrees of freedom. Moreover, owing to the fundamental nature of the model, the induced polarization of the Dirac-sea quarks has an intimate connection with the cloud of pions virtually excited around the core of three valence quarks inside the nucleon [12,13]. (The Skyrme model also takes account of such effects of pionic cloud. However, it has been argued that the lack of the valence quark concept in this model sometimes misses important physics [10,11].) This unique feature of the model should in principle be tested through observations.

In recent short articles [12,13], we have tried to clarify this deep connection between the pionic and sea-quark components in the nucleon through the analysis of various QCD phenomenology in the low-energy domain. The present paper is a more complete report of these studies, including the detail of the method of calculation as well as more thorough explanation of the physics behind. The paper is organized as follows. First, in Sec. II, we review the basic physics of the chiral quark soliton model. Although the material here has considerable overlap with that in our previous paper [8], we think it useful to understand the discussion in the following sections. Next, in Sec. III, the charge distributions of the nucleon (especially that of the neutron) are investigated with the special intention of revealing the role of the Dirac-sea quarks. This analysis demonstrates in the most transparent fashion that the effect of sea quarks incorporated in this model automatically simulates that of a pion cloud surrounding the core of three valence quarks. The electric form factors of the proton and the neutron are also calculated and compared with experimental data.

In Sec. IV, we investigate the quark condensate in the nucleon. We emphasize that the chiral quark soliton

model naturally predicts the spatially varying quark condensate inside the nucleon. It is demonstrated there that this local structure of the $\bar{q}q$ condensate can be understood as an interplay of the valence and sea quark degrees of freedom. The spatial integrals of the $\bar{q}q$ condensates are known to be related to interesting observables such as the πN Σ term etc. We shall calculate these quantities and compare them with the existing empirical information. We also try to obtain the separate knowledge of the $\bar{u}u$ and $\bar{d}d$ condensates, which turn out to give important information on the isospin asymmetry of the $q\bar{q}$ sea. In Sec. V, the physics of the Gottfried sum is shortly reviewed and our analysis based on the chiral quark soliton model is reported. Finally, some concluding remarks will be given in Sec. VI.

II. THE CHIRAL QUARK SOLITON MODEL

The chiral quark model is specified by the vacuum functional [2,8]

$$Z=\int \mathcal{D}\pi\,\mathcal{D}\psi\,\mathcal{D}\psi^{\dagger}\exp\left[i\int d^4x\,\bar{\psi}(i\partial\!\!\!/-MU^{\gamma_5}-m)\psi\right], \tag{2.1}$$

where

$$U(x)=e^{i\gamma_5\tau\cdot\pi(x)/f_\pi}. \tag{2.2}$$

Here $\psi(x)$ and $\pi(x)$ stand for the quark and pion fields, respectively. The absence of the kinetic term for the latter field implies that it is not an independent field of quarks, but is eventually interpreted as a composite field in the $q\bar{q}$ channel. In addition to the dynamical quark mass M, which is assumed to be generated through the spontaneous chiral-symmetry breaking of the QCD vacuum, here we have introduced a small but finite bare quark mass m, so as to reproduce the physical pion mass. (See below.) The effective quark mass in the physical vacuum ($U=1$) then becomes $\bar{M}=M+m$. Including an intrinsic physical cutoff Λ, the model contains four parameters: M, m, f_π, Λ. Throughout the study, we always set $f_\pi=93$ MeV. On the basis of the instanton picture of the QCD vacuum, Diakonov and Petrov argued that the reasonable value of M is around 350 MeV [2,3]. In the following, we regard it as an adjustable parameter within the range $M\simeq(350-450)$ MeV. (We recall that this parameter plays the role of the quark-pion coupling constant, which controls the character of the resultant soliton solution [3,8].) To determine the remaining parameters, we make use of the derivative (gradient) expansion technique for obtaining effective meson actions [14–19]. We require that the effective meson action derived from the vacuum functional (2.1) reproduces both the kinetic and mass terms of the pion field with the correct coefficients. To this end, let us first define the effective meson action $S_{\rm eff}[U]\equiv\int d^4x\,\mathcal{L}_{\rm eff}[U]$ by performing the path integration over the quark fields:

$$Z=\int \mathcal{D}\pi\, e^{iS_{\rm eff}[U]}. \tag{2.3}$$

This gives

$$S_{\rm eff}[U]=-iN_c\,{\rm Sp}\ln\left[\frac{(i\partial\!\!\!/-MU^{\gamma_5}-m)}{(i\partial\!\!\!/-M-m)}\right]. \tag{2.4}$$

The standard proper-time regularization means the replacement [14–19]

$$S_{\rm eff}[U]\to\frac{1}{2}iN_c\int_0^\infty\frac{d\tau}{\tau}\varphi(\tau){\rm Sp}[-e^{-D_0^\dagger D_0\tau}], \tag{2.5}$$

where

$$D^\dagger D=\partial^2+\bar{M}^2+mM(U^{\gamma_5}+U^{\gamma_5\dagger}-2)+iM\partial\!\!\!/U^{\gamma_5}, \tag{2.6}$$

$$D_0^\dagger D_0=\partial^2+\bar{M}^2. \tag{2.7}$$

Here $\varphi(\tau)$ is a cutoff function satisfying the condition $\varphi(0)=0,\varphi(\infty)=1$. By using the derivative expansion technique, it is easy to show that

$$\mathcal{L}_{\rm eff}[U]\sim\frac{1}{f_\pi^2}\left[\frac{N_cM^2}{4\pi^2}\int_0^\infty\frac{d\tau}{\tau}\varphi(\tau)e^{-\tau\bar{M}^2}\right]\frac{1}{2}(\partial_\mu\pi)^2 - \frac{4m}{f_\pi^2}\left[\frac{N_cM}{8\pi^2}\int_0^\infty\frac{d\tau}{\tau^2}\varphi(\tau)e^{-\tau\bar{M}^2}\right]\frac{1}{2}\pi^2+\cdots, \tag{2.8}$$

where only the lowest-order terms relevant for our argument below are explicitly shown. Requiring that this effective meson Lagrangian reproduces the kinetic and mass terms of the pion field with the correct coefficients, we are led to the two conditions

$$f_\pi^2=\frac{N_cM^2}{4\pi^2}\int_0^\infty\frac{d\tau}{\tau}\varphi(\tau)e^{-\tau\bar{M}^2}, \tag{2.9}$$

$$\frac{f_\pi^2m_\pi^2}{m}=\frac{N_cM}{2\pi^2}\int_0^\infty\frac{d\tau}{\tau^2}\varphi(\tau)e^{-\tau\bar{M}^2}. \tag{2.10}$$

[Here the misprint of Eq. (4) in Ref. [13] has been corrected.] Assuming the cutoff function of the simplest form $\varphi(\tau)=\theta(\tau-1/\Lambda^2)$ (which corresponds to Schwinger's proper-time cutoff in the original form), the above two relations can be used to determine Λ and m. Their numerical values are $\Lambda=1.85\bar{M}$, $1.71\bar{M}$, $1.59\bar{M}$, $1.50\bar{M}$, $1.42\bar{M}$, and $m=14.2$, 15.0, 15.7, 16.3, 16.8 MeV, respectively, for $M=350$, 375, 400, 425, 450 MeV. We have no freedom of taking other values of m, as far as we require that the pion mass is reproduced with the simplest choice $\varphi(\tau)=\theta(\tau-1/\Lambda^2)$ for the cutoff function. The resultant bare quark masses are about two times as large as the generally accepted value deduced from the current-algebra analysis, i.e., $\bar{m}\equiv\frac{1}{2}(m_u+m_d)\simeq7$ MeV [20]. This in turn means that the vacuum quark condensate is underestimated for the above choice of the regularization function. To see this, notice first that from Eq. (2.1), the vacuum quark condensate $\langle\bar{\psi}\psi\rangle_{\rm vac}\equiv\langle0|\bar{u}u+\bar{d}d|0\rangle$ can be obtained as

$$\langle\bar{\psi}\psi\rangle_{\rm vac}=\frac{\delta}{\delta m}(E_{\rm vac}[m]/V), \tag{2.11}$$

where

$$E_{\rm vac}[m]=8\frac{N_c}{4\sqrt{\pi}}\int_0^\infty\frac{d\tau}{\tau\sqrt{\tau}}\varphi(\tau)\sum_k e^{-\tau\epsilon_k^2}\ , \tag{2.12}$$

with $\epsilon_k=\sqrt{k^2+\overline{M}^2}$, $\overline{M}=M+m$. This gives

$$-\langle 0|\bar{u}u+\bar{d}d|0\rangle=\frac{N_c\overline{M}}{2\pi^2}\int_0^\infty\frac{d\tau}{\tau^2}\varphi(\tau)e^{-\tau\overline{M}^2}\ . \tag{2.13}$$

Combining Eq. (2.13) with Eq. (2.10), we then obtain

$$f_\pi^2 m_\pi^2=-\gamma m\langle 0|\bar{u}u+\bar{d}d|0\rangle\ , \tag{2.14}$$

with $\gamma=(1+m/M)^{-1}$. Except for the factor γ, which is thought to be a higher-order correction to the chiral perturbation theory (its numerical value is very close to 1), this is the celebrated Gell-Mann–Oakes–Renner relation [21]. It is known that since the left-hand side (LHS) of Eq. (2.14) depends only on physical observables, the product of the current quark mass and the vacuum quark condensate should be renormalization scale invariant. As pointed out above, the proper-time regularization scheme with the simplest choice $\varphi(\tau)=\theta(1-1/\Lambda^2)$ leads to larger bare quark mass as compared with the standard current algebra estimate. Consequently, the numerical value of the vacuum quark condensate is necessarily underestimated. Taking $M=375$ MeV, for example, we have $\langle 0|\bar{u}u|0\rangle=\langle 0|\bar{d}d|0\rangle=-(179\ \text{MeV})^3$, while the empirical estimate with $\overline{m}=7\pm2$ MeV gives $\langle 0|\bar{u}u|0\rangle=\langle 0|\bar{d}d|0\rangle=-(225\pm25\ \text{MeV})^3$ [20]. This problem could be circumvented by making use of the freedom of taking a more general form of the cutoff function $\varphi(\tau)$ [22]. For simplicity, here we use Schwinger's proper-time regularization function in the original form. [We shall report elsewhere on the cutoff function dependence of the final physical predictions, which turned out to be very weak once the above physical conditions (2.9) and (2.10) were imposed.] It should be emphasized that the derivative expansion is used only to fix the parameters of the model. We shall never use it to obtain the $B=1$ soliton solution. In fact, it is known that the effective meson action obtained by truncating the derivative expansion has no stable soliton solution.

Now let us briefly review how we can construct the physical nucleon and how we can calculate its properties on the basis of the effective action (2.1) [3]. We expect that this short review would be useful for the readers to understand how the isospin asymmetry in the $q\bar{q}$ sea in the nucleon arises in this extremely simple model and how it can be calculated in a nonperturbative manner. We start with a static pion field (mean-field) configuration of hedgehog shape as

$$U=e^{i\tau\cdot\hat{\mathbf{r}}F(r)}\ . \tag{2.15}$$

The quark field then obeys the Dirac equation

$$H|m\rangle=E_m|m\rangle\ , \tag{2.16}$$

with

$$H=\frac{\alpha\cdot\nabla}{i}+M\beta[\cos F(r)+i\gamma_5\tau\cdot\hat{\mathbf{r}}\sin F(r)]+m\beta\ . \tag{2.17}$$

The presence of the potential term proportional to $\tau\cdot\hat{\mathbf{r}}$ destroys both the angular momentum and isospin symmetry. That is, the above Dirac Hamiltonian commutes with neither the angular momentum operator J nor the isospin operator τ for quarks [23–26]. A linear combination of them, $K=J+\frac{1}{2}\tau$, called the grand spin, however, commutes with H. As a consequence, the eigenstates of H are specified by the parity, the magnitude of the grand spin, and its projection M_K as [26]

$$|m\rangle=|K^{\rm parity}M_K\rangle\ , \tag{2.18}$$

with $K^P=0^\pm,1^\pm,2^\pm,\ldots$. A characteristic feature of the above Dirac equation is that one deep single-quark bound state having the quantum number of $K^P=0^+$ appears from the positive-energy continuum [26]. We call it the valence quark orbital. An object with baryon number one with respect to the physical vacuum is obtained by putting $N_c(=3)$ quarks into this valence orbital as well as all the negative-energy (Dirac-sea) orbitals. (This $B=1$ object is sometimes called the quark hedgehog.) Accordingly, the total energy of this quark hedgehog is given as

$$E_{\rm static}[U]=N_cE_0[U]+E_{\rm VP}[U]\ . \tag{2.19}$$

Here E_0 represents the energy of the valence quark level, and therefore N_c times E_0 gives the valence quark contribution to the static energy. On the other hand, $E_{\rm VP}$ stands for the vacuum polarization contribution. Regularizing it in the proper-time scheme, we have

$$E_{\rm VP}[U]=\frac{N_c}{2}\frac{1}{\sqrt{4\pi}}\int_0^\infty\frac{d\tau}{\tau\sqrt{\tau}}\varphi(\tau)\left[\sum_m e^{-\tau E_m^2}-\sum_k e^{-\tau\epsilon_k^2}\right]\ . \tag{2.20}$$

The energy of the true ($U=1$) vacuum is subtracted here: ϵ_k is the eigenenergy of the unperturbed Hamiltonian $H_0\equiv H(U\to1)$. The most probable pion field configuration (the self-consistent Hartree field) is now determined on the basis of the stationary phase approximation [2–10]. Under the hedgehog assumption, this gives the extremum condition

$$\frac{\delta}{\delta F(r)}E_{\rm static}[U]=0\ . \tag{2.21}$$

By using the explicit form of $E_{\rm static}[U]$, this leads to the equation of motion

$$S(r)\sin F(r)=P(r)\cos F(r)\ , \tag{2.22}$$

with

$$S(r)=S_{\rm val}(r)+S_{\rm VP}(r)\ , \tag{2.23}$$

$$P(r)=P_{\rm val}(r)+P_{\rm VP}(r)\ , \tag{2.24}$$

where

$$S_{\rm val}(r)=N_c\left\langle 0\left|\frac{\gamma^0\delta(|\mathbf{x}|-r)}{r^2}\right|0\right\rangle\ , \tag{2.25}$$

$$S_{\rm VP}(r)=-\frac{N_c}{2}\sum_m g(E_m;\Lambda)\left\langle m\left|\frac{\gamma^0\delta(|\mathbf{x}|-r)}{r^2}\right|m\right\rangle\ , \tag{2.26}$$

and the corresponding expressions for $P_{\rm val}(r)$ and $P_{\rm VP}(r)$ are obtained from $S_{\rm val}(r)$ and $S_{\rm VP}(r)$ with the replacement of γ^0 by $i\gamma^0\gamma_5\tau\cdot\hat{\mathbf{r}}$. In Eq. (2.26), $g(E_m;\Lambda)$ is a regularization function given as

$$g(E_m;\Lambda)=\mathrm{sgn}(E_m)\mathrm{erfc}(|E_m|/\Lambda) , \tag{2.27}$$

which is obtained from the more general definition

$$g(E_m)=\frac{1}{\sqrt{\pi}}\int_0^\infty \frac{d\tau}{\sqrt{\tau}}\varphi(\tau)E_m e^{-\tau E_m^2} , \tag{2.28}$$

by making the special choice $\varphi(\tau)=\theta(1-1/\Lambda^2)$. Equation (2.22) combined with the Dirac equation (2.16) reduces to a self-consistent problem which will be solved by the iteration method [4–8]. After the satisfaction of self-consistency, the hedgehog pion field, which was originally treated as an external background field for quarks, becomes an implicit functional of the quark field.

The $B=1$ mean-field solution obtained as above cannot yet be identified with the physical nucleon, since it does not have good spin and isospin quantum numbers [2,8]. (The situation is entirely analogous to the classical solution of the Skyrme model [27,28].) This is due to the degeneracy of the soliton energy under the SU(2)-isospin rotation. To obtain a baryon state with good spin and isospin, this zero-energy mode must be quantized. It can be achieved by considering a time-dependent isorotation of the symmetry-breaking mean field [2,8]:

$$\tilde{U}(\mathbf{x},t)=A(t)U(\mathbf{x})A^\dagger(t) . \tag{2.29}$$

Here $U(\mathbf{x})$ is the stationary pion field configuration of hedgehog shape obtained before. $A(t)$ is a time-dependent SU(2) matrix characterizing a global rotation in isospace. By using Eq. (4.1), the Dirac operator $\tilde{D}\equiv i\partial\!\!\!/-M\tilde{U}^{\gamma_5}$ is expressed in the form

$$\tilde{D}=A(t)\gamma^0(i\partial_t-H+\Omega)A^\dagger(t) , \tag{2.30}$$

where H is the time-independent Hamiltonian introduced in the preceding section, while Ω is the collective angular velocity operator defined by

$$\Omega=iA^\dagger\dot{A}=\tfrac{1}{2}\Omega_a\tau_a , \tag{2.31}$$

with $\dot{A}=(d/dt)A(t)$. The quantity $i\partial_t-H+\Omega$ in Eq. (4.2) corresponds to the Dirac Hamiltonian in the isorotating system, and then $H-\Omega$ is the familiar cranking Hamiltonian with Ω the analogue of the Coriolis force [29]. To obtain the energy of the rotating soliton, we analyze the energy change of the quark hedgehog induced by the isorotation, by treating the Coriolis coupling as an external perturbation. The first nonvanishing correction to the static energy results from the second-order term in Ω. This leads to the expression for the energy of the quantized soliton with the definite angular momentum as [3,29]

$$E_J=E_{\rm static}+\frac{J(J+1)}{2I} . \tag{2.32}$$

Here I is the moment of inertia introduced through the quantization rule:

$$\Omega_a\to-\frac{\hat{J}}{I} . \tag{2.33}$$

It is given as a sum of the valence and vacuum polarization contributions:

$$I=I_{\rm val}+I_{\rm VP} , \tag{2.34}$$

with

$$I_{\rm val}=\frac{N_c}{2}\sum_{m\neq0}\frac{\langle0|\tau_3|m\rangle\langle m|\tau_3|0\rangle}{E_m-E_0} , \tag{2.35}$$

$$I_{\rm VP}=\frac{Nc}{8}\sum_{m,n}f(E_m,E_n;\Lambda)\langle n|\tau_3|m\rangle\langle m|\tau_3|n\rangle . \tag{2.36}$$

Here $|m\rangle$ denote the eigenstates of H, while $|0\rangle$ represents the valence quark level. The cutoff function $f(E_m,E_n;\Lambda)$ with the choice $\varphi(\tau)=\theta(1-1/\Lambda^2)$ is given as

$$f(E_m,E_n;\Lambda)=\frac{\mathrm{sgn}(E_m)\mathrm{erfc}(|E_m|/\Lambda)-\mathrm{sgn}(E_n)\mathrm{erfc}(|E_n|/\Lambda)}{E_m-E_n}-\frac{2}{\sqrt{\pi}}\Lambda\frac{e^{-E_m^2/\Lambda^2}-e^{-E_n^2/\Lambda^2}}{E_m^2-E_n^2} . \tag{2.37}$$

For more general form of $\varphi(\tau)$, this function should be replaced by

$$f(E_m,E_n)=-\frac{1}{\sqrt{\pi}}\int_0^\infty\frac{d\tau}{\sqrt{\tau}}\varphi(\tau)\left[\frac{E_m e^{-\tau E_m^2}+E_n e^{-\tau E_n^2}}{E_m+E_n}+\frac{1}{\tau}\frac{e^{-\tau E_m^2}-e^{-\tau E_n^2}}{E_m^2-E_n^2}\right] . \tag{2.38}$$

The induced Coriolis coupling, which generates a change in the intrinsic quark wave functions, also gives some influences on any physical quantities. These effects are again estimated under the assumption of slow isorotation, i.e., by truncating the power series expansion in Ω. Retaining terms up to the linear order in Ω, we are led to the following general formula which enables us to evaluate the nucleon (and Δ) matrix element of arbitrary quark bilinear operator $\bar{\psi}\hat{O}^\mu\psi$ [8]:

$$\langle J'J'_3T'_3|\hat{O}^\mu|JJ_3T_3\rangle=\int d\xi_A\Psi^{(J')*}_{J'_3T'_3}[\xi_A]O^\mu[\xi_A]\Psi^{(J)}_{J_3T_3}[\xi_A] , \tag{2.39}$$

where

$$\Psi^{(J)}_{J_3T_3}[\xi_A]=\left[\frac{2J+1}{8\pi^2}\right]^{1/2}(-1)^{T+T_3}D^{(J)}_{-T_3J_3}(\xi_A)\ , \tag{2.40}$$

is the wave function describing the collective isorotation of the quark hedgehog. The operator $O^\mu[\xi_A]$ is again given as a sum of the valence and vacuum polarization contributions:

$$O^\mu[\xi_A]=O^\mu_{\rm val}[\xi_A]+O^\mu_{\rm VP}[\xi_A]\ , \tag{2.41}$$

with

$$O^\mu_{\rm val}[\xi_A]\sim N_c\langle 0|A^\dagger\gamma^0\hat{O}^\mu A|0\rangle + N_c\sum_{m\neq 0}\left[\frac{1}{2}\Omega_a,\frac{\langle 0|\tau_a|m\rangle\langle m|A^\dagger\gamma^0\hat{O}^\mu A|0\rangle}{E_m-E_0}\right]_+\ , \tag{2.42}$$

$$O^\mu_{\rm VP}[\xi_A]\sim -\frac{N_c}{2}\sum_n g(E_m;\Lambda)\langle n|A^\dagger\gamma^0\hat{O}^\mu A|n\rangle + \frac{N_c}{4}\sum_{m,n}f(E_m,E_n;\Lambda)\left[\frac{1}{2}\Omega_a,\langle n|\tau_a|m\rangle\langle m|A^\dagger\gamma^0\hat{O}^\mu A|n\rangle\right]_+\ . \tag{2.43}$$

The physical meaning of the above formula can be easily understood from the schematic diagrams depicted in Fig. 1. Here Fig. 1(a) corresponds to the valence quark contribution $O^\mu_{\rm val}[\xi_A]$, whereas Fig. 1(b) to the vacuum polarization one $O^\mu_{\rm VP}[\xi_A]$. [To be more precise, owing to the introduction of the finite momentum cutoff, the second term of (2.43) contains some other minor contributions that do not correspond to the second diagram of Fig. 1(b).] All the physical quantities investigated in the following sections can be evaluated by using the above general formula together with the expression of the moment of inertia.

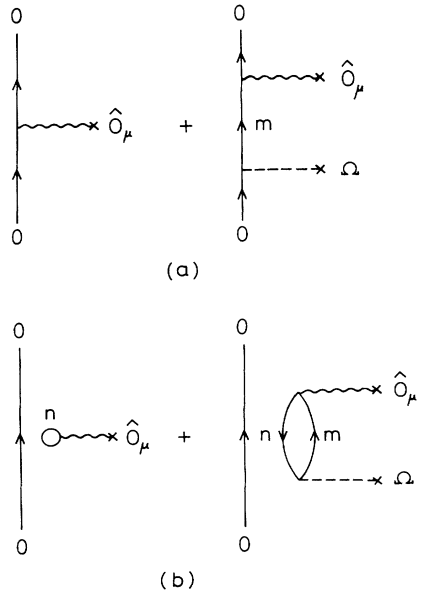

FIG. 1. The schematic diagrams representing the contributions to the matrix element of the operator $\bar{\psi}\hat{O}_\mu\psi$. (a) and (b), respectively, corresponds to the valence and vacuum quark contributions.

III. NUCLEON CHARGE DISTRIBUTIONS

We are interested here in the nucleon charge distributions [13]. The relevant quark bilinear operator is the charge density operator given by

$$\psi^\dagger(x)\left[\frac{1}{2N_c}+\frac{\tau_3}{2}\right]\psi(x)$$

with $N_c(=3)$ the independent color numbers of quarks. It is convenient to treat the isoscalar and isovector part separately. Owing to the peculiar hedgehog nature of the mean-field potential, the dominant contribution to the isoscalar part arises in the zeroth order in the collective angular velocity Ω [8], whereas the isovector part survives only in the first order in Ω. Consequently, the theoretical expression for these two quantities have rather dissimilar structure as shown below. First we show the formula for the isoscalar charge density:

$$\rho^{(I=0)}(r)=\rho^{(I=0)}_{\rm val}(r)+\rho^{(I=0)}_{\rm VP}(r)\ , \tag{3.1}$$

where

$$\rho^{(I=0)}_{\rm val}(r)=\left\langle 0\left|\frac{\delta(|\mathbf{x}|-r)}{r^2}\right|0\right\rangle\ . \tag{3.2}$$

$$\rho^{(I=0)}_{\rm VP}(r)=-\frac{1}{2}\sum_m g(E_m;\Lambda)\left\langle m\left|\frac{\delta(|\mathbf{x}|-r)}{r^2}\right|m\right\rangle\ . \tag{3.3}$$

Here $|m\rangle$ and E_m denote the eigenstates and associated eigenenergies of the single-quark Dirac equation (2.16).

The theoretical formula for the isovector charge is slightly more complicated. It is given in the form

$$\rho^{(I=1)}(r)=\rho^{(I=1)}_{\rm val}(r)+\rho^{(I=1)}_{\rm VP}(r)\ , \tag{3.4}$$

where

$$\rho_{\rm val}^{(I=1)}(r)=\frac{1}{I}\frac{N_c}{2}\sum_{m\neq 0}\frac{1}{E_m-E_0}\langle 0|\tau_3|m\rangle\left\langle m\left|\tau_3\frac{\delta(|\mathbf{x}|-r)}{r^2}\right|0\right\rangle , \tag{3.5}$$

$$\rho_{\rm VP}^{(I=1)}(r)=\frac{1}{I}\frac{Nc}{8}\sum_{m,n}f(E_m,E_n;\Lambda)\langle n|\tau_3|m\rangle\left\langle m\left|\tau_3\frac{\delta(|\mathbf{x}|-r)}{r^2}\right|n\right\rangle . \tag{3.6}$$

Here I is the moment of inertia of the soliton that appears through the quantization procedure of the collective iso-rotation.

The numerical algorithm of Kahana and Ripka ensures practical utility of the above formulas [26]. Following them, the plane-wave basis, introduced as a set of eigenstates of the free Hamiltonian $H_0=\boldsymbol{\alpha}\cdot\nabla/i+\beta(M+m)$, is discretized by imposing an appropriate boundary condition for the radial wave functions at the radius D chosen to be sufficiently larger than the soliton size. The basis is made finite by including only those states with the momentum k as $k<k_{\rm max}$. The eigenvalue problem (2.16) is then solved by diagonalizing the Dirac Hamiltonian H in the above basis. We are thus able to solve the self-consistent Hartree problem and also to calculate any nucleon observables with full inclusion of the sea-quark degrees of freedom. The stability of the final answer against further increase of D and $k_{\rm max}$ has been carefully checked.

This numerical method works remarkably well for the calculation of the isoscalar charge density [4–7]. According to the classification in Ref. [8], this isoscalar charge density operator is that of the first type. The vacuum polarization contribution to such quantities can be calculated by performing a single sum of the diagonal matrix element over all the quark orbitals. On the other hand, in order to calculate the vacuum polarization contribution to the isovector charge density (this is an operator of the second type), we must perform a double sum of the product of the nondiagonal matrix element. As was explained in Ref. [8], the calculation of such quantities is rather involved, because of the mixture of the "spurious" vacuum contribution resulting from the unphysical boundary effect of the plane-wave basis of Kahana and Ripka. The detailed analysis described in Ref. 8 shows that a simple subtraction procedure

$$I_{\rm VP}\rightarrow I_{\rm VP}-I_{\rm VP}\quad(U=1) \tag{3.7}$$

works well in the calculation of the moment of inertia. In the present problem, this means the replacement

$$\rho_{\rm VP}^{(I=1)}(r)\rightarrow\rho_{\rm VP}^{(I=1)}(r)-\rho_{\rm VP}^{(I=1)}\quad(r;U=1) . \tag{3.8}$$

In a recent paper, Goeke *et al.* proposed another simple prescription for eliminating "unphysical" vacuum contribution to the moment of inertia [30]. According to them, the problem is circumvented by rewriting the matrix element $\langle n|\tau_3|m\rangle$ as

$$\langle n|\tau_3|m\rangle=\frac{\langle n|[H,\tau_3]|m\rangle}{E_n-E_m} , \tag{3.9}$$

and evaluating the right-hand side. Here it should be understood that the matrix element in the RHS is calculated after analytically evaluating the commutator. We have verified that this method and our previous method give the same answer within 1% for large enough values of D and $k_{\rm max}$. This new method due to Goeke *et al.* however seems to be superior in the case we need to calculate quantities having slowly damping tail such as the isovector square charge radius. As pointed out by them, this is probably because the analytical evaluation of the commutator $[H,\tau_3]$ introduces a natural cutoff at long distances larger than the soliton size and the unphysical boundary effects are removed. We solved the self-consistent Hartree problem for several values ranging from 350 to 450 MeV. The calculation here introduces a finite bare quark mass m, which was discarded in our previous paper [8]. We show in Table I, the theoretical prediction for the moment of inertia as a function of the dynamical quark mass M. The corresponding values for the $N\Delta$ mass difference, which are given as $3/2I$, are also shown. One sees that the moment of inertia is a decreasing function of the mass parameter M [8,30]. The choice $M\simeq 425$ MeV approximately reproduces the $N\Delta$ mass difference. We however think it premature to regard it as the most favorable value for the model parameter M. It may be safer to think that this gives an upper bound for M, since the residual one-gluon-exchange interaction (not fully incorporated into the Lagrangian of the chiral quark model) might also contribute to the $N\Delta$ mass difference.

Shown in Fig. 2 are the isoscalar (a) and isovector (b) charge densities. (These figures as well as Figs. 3 and 4 are taken from Ref. 13.) In both figures, the dotted and dash-dotted curves stand for the valence and vacuum po-

TABLE I. The moment of inertia and the $N-\Delta$ mass difference as functions of M.

M (MeV)	$I_{\rm val}$	$I_{\rm VP}$	$I_{\rm total}$	$M_\Delta-M_N$ (MeV)
350	0.00755	0.00113	0.00868	173
375	0.00567	0.00121	0.00688	218
400	0.00470	0.00126	0.00596	252
425	0.00405	0.00128	0.00533	281
500	0.00357	0.00130	0.00487	308

larization contributions, while their sum is shown by the solid curve. One immediately finds that the vacuum polarization contribution to the isoscalar charge density is very small for the self-consistent solution obtained here [5,7]. On the contrary, the vacuum polarization effect on the isovector charge density turns out to be appreciable. In particular, it dominates over the valence quark contribution for $r > 1.5$ fm. It is also instructive to examine the integrated charge. The spatial integral of Eq. (10) gives

$$\int_0^\infty dr\, r^2 \rho^{(I=1)}(r) = \frac{I_{\rm val}}{I} + \frac{I_{\rm VP}}{I} , \tag{3.10}$$

where the first and the second terms on the RHS, respectively, correspond to the valence and vacuum polarization contributions to the isovector charge. (Their sum is unity since $I = I_{\rm val} + I_{\rm VP}$, where $I_{\rm val}$ and $I_{\rm VP}$ are, respectively, the valence and vacuum polarization contributions to the total moment of inertia.) Numerically, we find $I_{\rm VP}/I \simeq 0.24$ for $M = 425$ MeV. (See Table II for the predictions for other values of M.) This roughly means that about 24% of the nucleon isovector charge (or the isospin) is carried by the Dirac-sea quarks. It should be contrasted with the fact that the isoscalar charge or the baryon number totally comes from the valence quarks. This last statement is not very precise, however. Because of the introduction of a finite cutoff, the vacuum polarization contribution to the isoscalar charge does not vanish exactly. The reason is as follows. Under the presence of the *CP*-violating static mean-field of hedgehog shape, the energy spectrum of the Dirac equation is generally asymmetric with respect to the positive and negative energies (the so-called spectral asymmetry). In the infinite cutoff limit of $\Lambda \to \infty$, the integrated vacuum charge reduces to

$$\int_0^\infty dr\, r^2 \rho_{\rm VP}^{(I=0)}(r) \to -\frac{1}{2}\sum_m {\rm sgn}(E_m) , \tag{3.11}$$

which counts the difference between the numbers of the positive- and negative-energy levels [31,32]. Assuming that the valence level lies in the energy range $0 < E_0 < M$ [which means that no single quark level crosses zero energy as the background potential $U(x)$ is adiabatically changed from the vacuum value ($U = 1$) to the self-consistent one], the RHS of Eq. (3.11) is clearly zero.

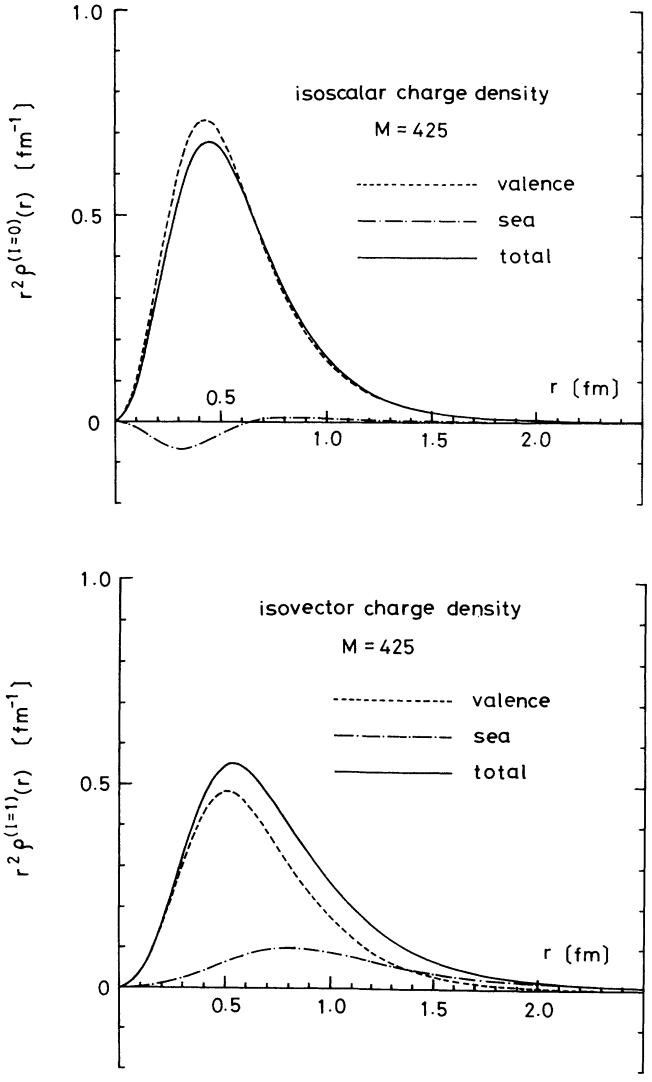

FIG. 2. The nucleon isoscalar (a) and isovector (b) charge densities calculated with the dynamical quark mass parameter $M = 425$ MeV. The dotted and dash-dotted curves, respectively, stand for the valence and vacuum polarization contributions, while the solid curve represents their sum.

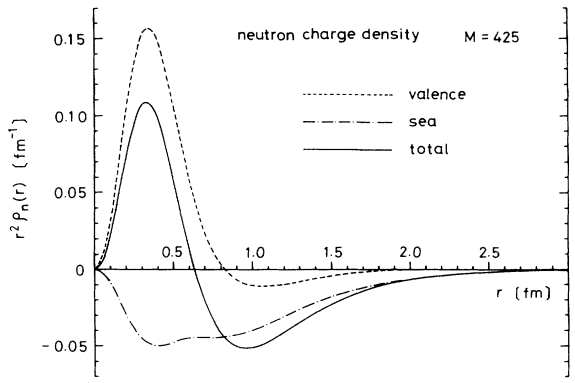

FIG. 3. The neutron charge density with $M = 425$ MeV. The curves have the same meaning as in Fig. 2.

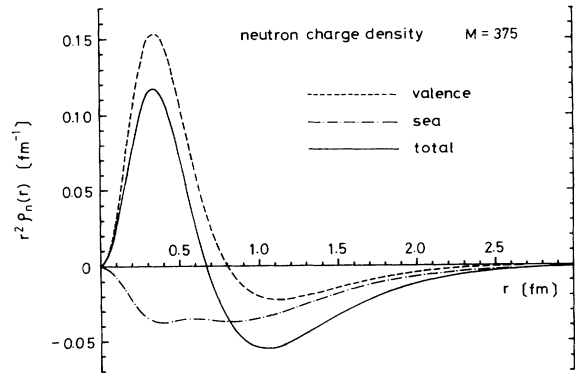

FIG. 4. The neutron charge density with $M = 375$ MeV. The curves have the same meaning as in Fig. 2.

TABLE II. The isovector charge as a function of M.

M (MeV)	Valence	Sea	Total
350	0.870	0.130	1.000
375	0.824	0.176	1.000
400	0.789	0.211	1.000
425	0.759	0.241	1.000
450	0.733	0.267	1.000

However, the introduction of a finite cutoff combined with the above spectral asymmetry necessarily lead to nonvanishing vacuum polarization contribution to the isoscalar charge (or the baryon number). This physically undesirable consequence cannot be avoided as far as a cutoff of finite value is introduced. The question is then whether or not it is intolerably large. We show in Table III the detailed contents of the theoretical isoscalar charge as functions of M. The problematical vacuum polarization contribution to the isoscalar charge grows with M. This is only natural, since the spectral asymmetry becomes larger as the quark-pion coupling constant M increases. The degrees of the violation of the baryon number is not extremely large even for the largest value of M. It is (2.2–3.6) % for the favorable range of the model parameter, i.e., $M=(375–425)$ MeV, and can be safely neglected as compared with the precision of the model itself.

Returning again to the comparison of the isoscalar and isovector charge densities, what is the physical explanation of the remarkable difference between these two? The answer lies in the old day's meson theory of the nucleon. This tells us that the isovector charge density receives large pionic effect, whereas the effect would be less important for the isoscalar density. (The pion is an isovector meson.) As emphasized in our previous paper [8], the vacuum polarization contribution in our chiral quark soliton model simulates such pionic effects, since the pionic degrees of freedom are incorporated as a composite $q\bar{q}$ field that takes the form of the background potential for quarks. Further support to this interpretation may be obtained by investigating the neutron charge distribution shown in Fig. 3. (It is obtained as the difference of the isoscalar and isovector charge density, i.e., $\rho^{(n)}(r)=\frac{1}{2}[\rho^{(I=0)}(r)-\rho^{(I=1)}(r)]$, so that a drastic cancellation occurs between the valence quark contributions to the isoscalar and isovector charge densities.) The dominant role of the vacuum polarization contribution, especially at large distances, is almost self-explanatory. In particular, it gives a sizable negative contribution to the charge density. This is certainly interpreted as simulating the effects of negatively charged pion cloud generated through the virtual dissociation process $n\rightarrow p+\pi^-$ at the nucleon level of $d\rightarrow u+\pi^-$ at the quark level. (In the quark level description, the virtual dissociation process $u\rightarrow d+\pi^+$ is also expected to occur. Note however that the neutron contains two d quarks and one u quark as valence particles.) To see the M dependence of the above result, we also show in Fig. 4 the neutron charge distribution for a slightly smaller value of M, i.e., $M\simeq 375$ MeV. A qualitative feature is unchanged, although the effect of sea quarks is somewhat less drastic as compared with the case of $M=425$ MeV.

TABLE III. The isoscalar charge (or baryon number) as a function of M.

M (MeV)	Valence	Sea	Total
350	1.000	−0.015	0.985
375	1.000	−0.022	0.978
400	1.000	−0.029	0.971
425	1.000	−0.036	0.964
450	1.000	−0.045	0.955

Now that all the relevant charge densities are given, it is quite easy to calculate the square charge radii of the nucleon which can be compared with the existing empirical data. As noted above, since the isoscalar charge density is not properly normalized to unity after including the vacuum polarization contribution, we have renormalized it as $\rho^{(I=0)}(r)\rightarrow Z\rho^{(I=0)}(r)$. [This tentative prescription is used also in calculating the isoscalar electric form factor. An alternative prescription is to use (without justification) the unregularized expression for $\rho^{(I=0)}(r)$ which is finite and only slightly different from the regularized one.] The numerical values of Z are 1.022 and 1.038, respectively, for $M=375$ and 425 MeV. It is equivalent to evaluating the isoscalar square charge radius $\langle r^2\rangle_{I=0}$ as

$$\langle r^2\rangle_{I=0}=\frac{\int_0^\infty dr\, r^4\rho^{(I=0)}(r)}{\int_0^\infty dr\, r^2\rho^{(I=0)}(r)}\ . \tag{3.12}$$

Table IV shows the theoretical isoscalar and isovector square charge radii as well as the square charge radii of the proton and neutron. One sees that the best agreement between the theory and experiment is obtained with the dynamical quark mass parameter around $M\simeq 375$ MeV. To see it more carefully, however, we find that there is no parameter M which reproduces the isoscalar and isovector charge radii simultaneously. If the isoscalar radius is reproduced, the isovector one is overestimated. On the other hand, if the isovector radius is reproduced, the isoscalar one is underestimated. We suspect that the problem lies in the isoscalar radius. In the well-known vector-meson-dominance (VMD) picture, the external photon couples to the isoscalar charge through the ω meson. Then, if one introduces the ω-meson de-

TABLE IV. The isoscalar and isovector square charge radii and the square charge radii of the proton and the neutron in dependence of M. All entries in $[fm^2]$. For the experimental numbers see [38] and references therein.

M (MeV)	$\langle r^2\rangle_{I=0}$	$\langle r^2\rangle_{I=1}$	$\langle r^2\rangle_p$	$\langle r^2\rangle_n$
350	0.723	1.098	0.910	−0.188
375	0.583	0.903	0.743	−0.160
400	0.512	0.826	0.669	−0.157
425	0.464	0.768	0.616	−0.152
500	0.428	0.727	0.578	−0.150
Experiment	0.62	0.86	0.74	−0.12

grees of freedom into the chiral quark Lagrangian, the isoscalar charge radius may be replaced by [17,19]

$$\langle r^2\rangle_{I=0} \rightarrow \frac{6}{m_\omega^2} + \langle r^2\rangle_{I=0} \ . \tag{3.13}$$

Here $\langle r^2\rangle_{I=0}$ in the RHS is the square radius of the core without the VMD mechanism. It has been pointed out by several authors that this ω-meson contribution offers a possibility to explain the isoscalar charge radius with rather small intrinsic core radius [33,34]. It is interesting to investigate this problem in the generalized chiral quark soliton model which minimally introduces the ω-meson degrees of freedom [35]. One might raise a question why the isovector charge radius is not also increased by the similar ρ-meson-dominance mechanism. A possible answer may be as follows: the 2π correlation having the quantum number of ρ meson is already incorporated into the model more efficiently than the 3π correlation simulating the effect of the ω meson. We can expect this, for example, from the experience of the analysis of the nuclear forces based on the Skyrme model [36,37]. The definite conclusion will of course be obtained only after investigating the model which includes all these freedom.

In Table V, we show more detailed contents of the square charge radii for several values of M. Crucial importance of the sea-quark contribution to the isovector radius is evident. Naturally, its effect is most drastic for the neutron charge radius. However, even the proton square charge radius receives a sizable sea-quark contribution. Large effects of sea quarks (or the effect of pion cloud) on the square radius is due to its dominance in the long-range region.

In Fig. 5, we show the theoretical predictions for the proton electric form factor (it is a Fourier transform of the charge distribution) together with the semiempirical fit of Gari and Krümpelmann [38]. A good agreement is seen to be obtained for the parameter $M \simeq (375-425)$ MeV. In Fig. 6, the theoretical prediction for the neutron electric form factor is compared with the recent experimental data by Platchkov *et al.* [39]. The theory appears to overestimate the experimental data in the whole momentum transfer ranges. This is probably related to our previous observation that the difference between the isoscalar and isovector charge radius is overestimated by the present model. It should be noted, however, that the experimental uncertainties are very large for the neutron form factor. In fact, it was determined through the analysis of the electron scatterings on the deuteron target, and is strongly dependent on the theoretical model (especially on the nucleon-nucleon potential) used in the analysis. The experimental data in Fig. 6 were obtained by Platchkov *et al.* with use of the Paris NN potential

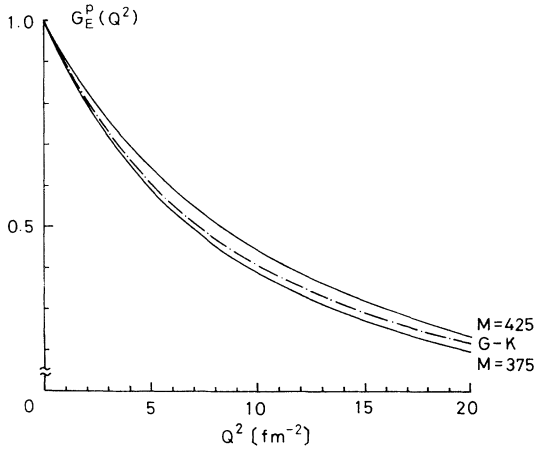

FIG. 5. The theoretical proton electric form factors with $M=375$ and 425 MeV in comparison with the semiempirical fit by Gari and Krümpelmann.

TABLE V. The detailed contents of the square charge radii in dependence of M.

M (MeV)	Contents	$\langle r^2\rangle_{I=0}$	$\langle r^2\rangle_{I=1}$	$\langle r^2\rangle_p$	$\langle r^2\rangle_n$
	Valence	0.676	0.875	0.775	−0.100
350	sea	0.047	0.223	0.135	−0.088
	total	0.723	1.098	0.910	−0.188
	Valence	0.534	0.629	0.582	−0.047
375	sea	0.049	0.274	0.161	−0.113
	total	0.583	0.903	0.743	−0.160
	valence	0.462	0.506	0.484	−0.022
400	sea	0.050	0.320	0.185	−0.135
	total	0.512	0.826	0.669	−0.157
	valence	0.414	0.426	0.420	−0.006
425	sea	0.050	0.342	0.196	−0.146
	total	0.464	0.768	0.616	−0.152
	valence	0.378	0.369	0.374	0.005
450	sea	0.050	0.358	0.204	−0.155
	total	0.428	0.727	0.578	−0.150
Experiment		0.62	0.86	0.74	−0.12

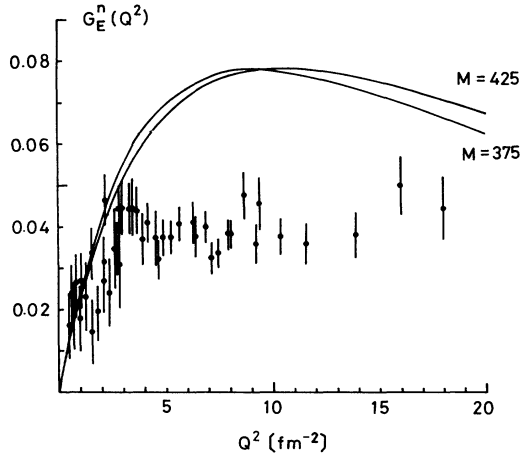

FIG. 6. The theoretical neutron electric form factors in comparison with the experimental data by Platchkov *et al.* The theoretical curves corresponds to $M=375$ and 425 MeV, whereas the experimental data are obtained through the analysis of the electron-deuteron scatterings by using the *NN* potential model of Platchkov *et al.*

[39]. To show the size of these uncertainties, we show in Fig. 7 the two-parameter fit of the neutron electric form factors obtained with other *NN* potential models [39] together with the Gari and Krümpelmann fit [38]. One confirms that the uncertainties are very large. More precise determination of the neutron electric form factor as well as the square charge radius is highly desirable.

IV. THE FLAVOR STRUCTURE OF THE QUARK CONDENSATE

An interesting feature of the chiral quark soliton model is that it naturally predicts the spatially varying $\bar{q}q$ condensate inside the nucleon. This local structure, which

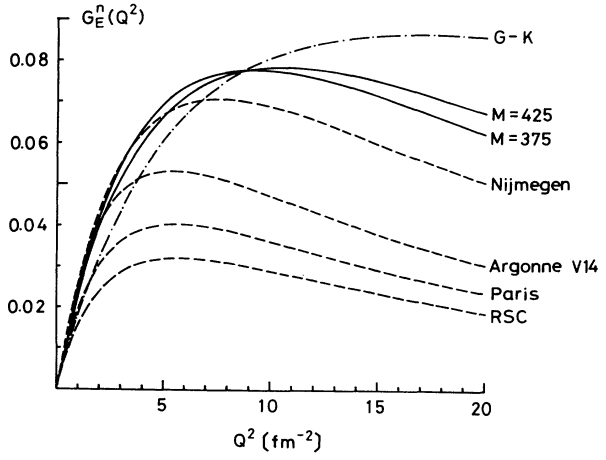

FIG. 7. The model dependence of the neutron electric form factor obtained by Platchkov *et al.* Their two-parameter fits with different *NN* potential models, i.e., the Paris, Reid soft-core, Argonne V14, and Nijmegen *NN* potentials, are shown by dashed curves. Also shown by the dash-dotted curve is the Gari and Krümpelmann fit. The theoretical curves are shown by the solid curves.

may be thought to be a kind of defect in the homogeneous vacuum quark condensate is of course generated by the presence of $N_c(=3)$ valence quarks contained in it. This physically apparent fact can be explicitly verified through our model analysis below. Let us first study the $\bar{q}q$ scalar condensate density $S^{(I=0)}(r)$ of isoscalar type. It is easily obtained by evaluating the nucleon matrix element of the quark bilinear operator $\bar{\psi}(x)\psi(x)$. Note however that this isoscalar scalar condensate density has already appeared in the process of solving the meanfield equation. That is, one immediately notices that $S^{(I=0)}(r)=S(r)$, where $S(r)$ is defined in Eqs. (2.23)–(2.26). By using these formulas, we can then separate the contributions of the valence and sea quarks to this scalar density. Figure 8 shows the result obtained with the solution of the self-consistent Hartree problem with the mass parameter $M=375$ MeV. The dashed and dash-dotted curves here, respectively, represent the valence and sea-quark contributions to the isoscalar scalar density, while their sum is shown by the solid curve. One clearly confirms that the valence quarks really works as a kind of impurity in the translational invariant QCD vacuum.

In order to obtain independent knowledge of the $\bar{u}u$ and $d\bar{d}$ scalar condensate, we need the isovector scalar condensate density in addition to the isoscalar one. We find that in the chiral quark soliton model the isovector scalar condensate survives only in the first order in Ω. Accordingly, its theoretical expression is slightly more complicated than that of the isoscalar one. It is given as

$$S^{(I=1)}(r)=S_{\rm val}^{(I=1)}(r)+S_{\rm VP}^{(I=1)}(r) , \tag{4.1}$$

where

$$S_{\rm val}^{(I=1)}(r)=\frac{1}{I}\frac{N_c}{2}\sum_{m\neq 0}\frac{1}{E_m-E_0}\langle 0|\tau_3|m\rangle \times\left\langle m\left|\gamma^0\tau_3\frac{\delta(|\mathbf{x}|-r)}{r^2}\right|0\right\rangle , \tag{4.2}$$

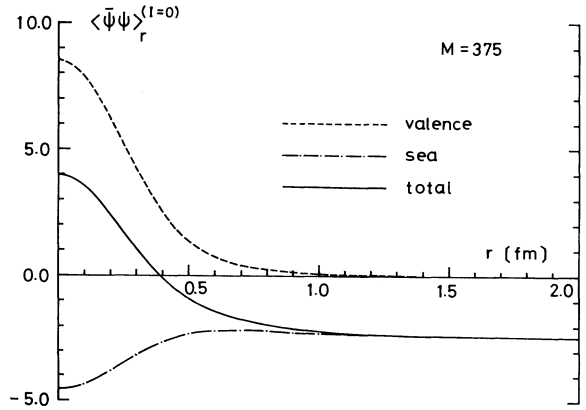

FIG. 8. The isoscalar scalar condensate density with $M=375$ MeV. The dashed and dash-dotted curves, respectively, stand for the valence and vacuum polarization contributions, while the solid curves represents their sum.

$$S_{\rm VP}^{(I=1)}(r)=\frac{1}{I}\frac{Nc}{8}\sum_{m,n}f(E_m,E_n;\Lambda)\langle n|\tau_3|m\rangle \times\left\langle m\left|\gamma^0\tau_3\frac{\delta(|\mathbf{x}|-r)}{r^2}\right|n\right\rangle . \quad (4.3)$$

Once both of $S^{(I=0)}(r)$ and $S^{(I=1)}(r)$ are given, the $\bar{u}u$ and $\bar{d}d$ scalar condensate densities in the proton are obtained as

$$\langle\bar{u}u\rangle_r\equiv\tfrac{1}{2}[S^{(I=0)}(r)+S^{(I=1)}(r)] , \quad (4.4)$$

$$\langle\bar{d}d\rangle_r\equiv\tfrac{1}{2}[S^{(I=0)}(r)-S^{(I=1)}(r)] . \quad (4.5)$$

The corresponding densities in the neutron are obtained by changing the sign of $S^{(I=1)}(r)$. (Since the present model assumes the degenerate mass for the u and d quarks, isospin symmetry is exact, or the neutron is an exact isospin partner of the proton.)

We show in Fig. 9 the theoretical isovector scalar condensate density in comparison with the isoscalar one. (The isoscalar scalar density here is with respect to the vacuum value.) The theoretical curves here corresponds to the soliton solution with $M=375$ MeV. One sees that the isovector scalar density is much smaller in magnitude than the isoscalar one (i.e., the isoscalar dominance of the scalar condensate). This equivalently means that there is not so much difference between the magnitudes of the $\bar{u}u$ and $\bar{d}d$ condensates as expected from the asymmetry of the valence quark numbers in the nucleon. (See Fig. 10.) We claim that the above isoscalar dominance of the scalar condensate has some phenomenological support. For showing this, it is better to study the spatial integrals of the above condensate densities. We recall that, when one talks about the quark condensates in the nucleon, one usually means these integrated quantities. For instance, the $\bar{u}u$ condensate in the proton $\langle p|\bar{u}u|p\rangle$ is obtained as the integral

$$\langle p|\bar{u}u|p\rangle\equiv\int_0^\infty dr\,r^2[\langle\bar{u}u\rangle_r-\langle\bar{u}u\rangle_{r=\infty}] , \quad (4.6)$$

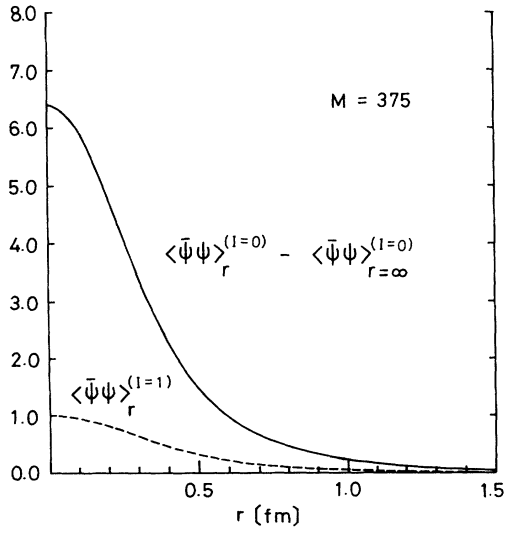

FIG. 9. The isovector scalar condensate density in comparison with the isoscalar one. The curves are obtained with $M=375$ MeV.

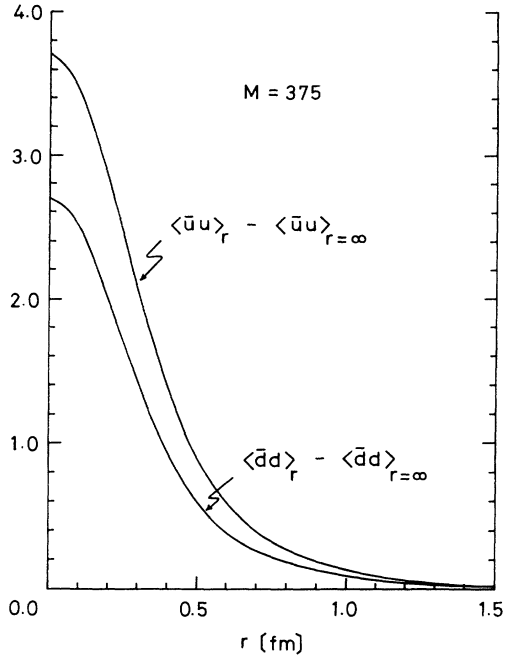

FIG. 10. The $\bar{u}u$ and $\bar{d}d$ scalar condensate densities with $M=375$ MeV.

with the similar expression for the $\bar{d}d$ condensate. Here $\langle\bar{u}u\rangle_{r=\infty}$ means the value of the $\bar{u}u$ condensate in the spatial infinity (i.e., the vacuum value). We show in Table VI, the theoretical predictions for the isoscalar and isovector condensates in the proton, i.e., $\langle p|\bar{u}u+\bar{d}d|p\rangle$ and $\langle p|\bar{u}u-\bar{d}d|p\rangle$, as functions of the dynamical quark mass M. One sees that the values of isovector scalar condensate are order of magnitude smaller than those of isoscalar one. Let us now compare this prediction with the phenomenology of low-energy QCD [13].

As is well known, the isoscalar combination of the $\bar{u}u$ and $\bar{d}d$ condensates is related to the πN Σ term through the relation

$$\Sigma=\bar{m}\langle p|\bar{u}u+\bar{d}d|p\rangle . \quad (4.7)$$

Here $\bar{m}$ is the average of the u- and d-quark masses. (We have set $m_u=m_d=m$, so that $\bar{m}=m$.) The numerical value of Σ has been a cause of controversy. Its estimate ranges from 30 to 60 MeV, with the first value arising from a fit of baryon mass formulas (under the assumption that the nucleon contains no $s\bar{s}$ component) and the second value coming from an analysis of low-energy pion nucleon scattering [20]. These values of the πN Σ term are compared with the theoretical predictions shown in the fifth column of Table VI. The agreement is satisfactory, although both the experimental and theoretical uncertainties are still very large. Also interesting is the difference between the $\bar{u}u$ and $\bar{d}d$ condensates, which is known to be related to the proton-neutron mass difference as [20,40]

$$(M_p-M_n)_{\rm QCD}=(m_u-m_d)\langle p|\bar{u}u-\bar{d}d|p\rangle . \quad (4.8)$$

Here $(M_p-M_n)_{\rm QCD}$ means the proton-neutron mass difference of purely QCD origin. That is, it is obtained

TABLE VI. The flavor contents of the $q\bar{q}$ scalar condensates in the proton as functions of M.

M (MeV)	$\langle p\|\bar{u}u+\bar{d}d\|p\rangle$	$\langle p\|\bar{u}u-\bar{d}d\|p\rangle$	$\langle p\|\bar{u}u\|p\rangle/\langle p\|\bar{d}d\|p\rangle$	Σ (MeV)
350	3.03	0.584	1.48	43.0
375	2.78	0.498	1.44	41.9
400	2.56	0.444	1.42	40.3
425	2.36	0.404	1.41	38.5
500	2.18	0.371	1.41	36.7

from the observed mass difference by correcting the electromagnetic effects:

$$(M_p-M_n)_{\rm QCD}=(M_p-M_n)_{\rm expt}-(M_p-M_n)_{\rm em} . \tag{4.9}$$

Using the theoretical estimate $(M_p-M_n)_{\rm em}\simeq 0.76$ MeV [20], this gives $(M_p-M_n)_{\rm QCD}\simeq -2.0$ MeV. Taking $m_u\simeq 5.1$ MeV and $m_d\simeq 8.9$ MeV, we then obtain

$$\langle p|\bar{u}u-\bar{d}d|p\rangle\simeq 0.526 . \tag{4.10}$$

This value is roughly consistent with our theoretical prediction given in the third column of Table VI, especially around $M\simeq 375$ MeV. The dominance of the isoscalar scalar condensate relative to the isovector one in the nucleon therefore seems to win a phenomenological support.

It may be also interesting to look at the same physics in a different way. Combining Eqs. (4.7) and (4.8), and using $(m_d-m_u)/(m_d+m_u)\simeq 0.27$, we obtain

$$r=\frac{\langle p|\bar{u}u|p\rangle}{\langle p|\bar{d}d|p\rangle}\simeq 1.13 \text{ to } 1.28 , \tag{4.11}$$

where the lower and upper values corresponds to taking $\Sigma=60$ and 30, MeV, respectively. We point out that the additivity rule $\langle p|\bar{u}u|p\rangle\simeq\langle p|u^\dagger u|p\rangle, \langle p|\bar{d}d|p\rangle\simeq\langle p|d^\dagger d|p\rangle$ which would mean $r=2$, is badly broken. (Notice that the quark-number-conservation law means $\langle p|u^\dagger u|p\rangle=2$, and $\langle p|d^\dagger d|p\rangle=1$.) The theoretical predictions for the ratio r in the chiral quark soliton model is shown in the fourth column of Table VI. They are slightly larger than the above semiempirical estimate, but certainly reproduces the tendency of the phenomenology in that they are definitely much smaller than 2. The enhanced $\bar{d}d$ condensate relative to the $\bar{u}u$ one in the proton already indicates isospin asymmetry of the $q\bar{q}$ sea in the nucleon. To see this more clearly, let us examine the prediction of our model in more detail. For example, with $M=375$ MeV, we have

$$\langle p|\bar{u}u|p\rangle_{\rm VP}/\langle p|\bar{u}u|p\rangle_{\rm val}=0.37 , \tag{4.12}$$

$$\langle p|\bar{d}d|p\rangle_{\rm VP}/\langle p|\bar{d}d|p\rangle_{\rm val}=0.64 . \tag{4.13}$$

These theoretical numbers imply the enhancement of the $d\bar{d}$ sea relative to the $u\bar{u}$ one in the proton, although they are not such quantities as directly observable.

V. THE GOTTFRIED SUM

Far more direct evidence for the suggested isospin-asymmetric sea has recently been obtained by the New Muon Collaboration (NMC) [41]. They investigated deep-inelastic muon scatterings on hydrogen and deuterium targets, and extracted the so-called Gottfried sum defined as

$$S_G=\int_0^1 dx\frac{F_2^p(x)-F_2^n(x)}{x} , \tag{5.1}$$

where $F_2^p(x)$ and $F_2^n(x)$ are the structure functions of the proton and the neutron, respectively. In the quark-parton model, $F_2(x)$ is expressed in terms of the quark momentum distribution functions $q_i(x)$, and the Gottfried sum is given by [42]

$$S_G=\int_0^1 dx\sum_i e_i^2\{q_i^p(x)+\bar{q}_i^p(x)-q_i^n(x)-\bar{q}_i^n(x)\} , \tag{5.2}$$

where e_i is the charge of a quark of flavor i. Assuming that the proton and the neutron form an isospin doublet, the quark distribution functions in the proton and those in the neutron can be related as

$$u^p(x)=d^n(x)\equiv u(x) , \quad d^p(x)=u^n(x)\equiv d(x) , \quad s^p(x)=s^n(x)\equiv s(x), \ldots , \tag{5.3}$$

(The isospin invariance is expected to be a reasonable assumption, since the mass difference of the u and d quarks is negligibly small as compared with the typical mass scale of hadron physics. See however the discussion below.) The Gottfried sum then becomes

$$S_G=\frac{1}{3}\int_0^1 dx[u(x)+\bar{u}(x)-d(x)-\bar{d}(x)] . \tag{5.4}$$

One may further separate the quark distributions into the valence and sea components as

$$u(x)=[u(x)-\bar{u}(x)]+\bar{u}(x)\equiv u_V(x)+u_S(x) , \tag{5.5}$$

$$d(x)=[d(x)-\bar{d}(x)]+\bar{d}(x)\equiv d_V(x)+d_S(x) . \tag{5.6}$$

Then, by using the standard sum rules [42]

$$\int_0^1 dx\, u_V(x)\equiv\int_0^1 dx[u(x)-\bar{u}(x)]=2 , \tag{5.7}$$

$$\int_0^1 dx\, d_V(x)\equiv\int_0^1 dx[d(x)-\bar{d}(x)]=1 , \tag{5.8}$$

for the valence quark distributions, we can also express S_G as

$$S_G=\frac{1}{3}+\frac{2}{3}\int_0^1 dx\{\bar{u}(x)-\bar{d}(x)\} . \tag{5.9}$$

Now assume that the $q\bar{q}$ sea in the proton is flavor (isospin) symmetric ($\bar{u}=\bar{d}$). The expected answer for S_G is then 1/3 (the Gottfried sum rule). Experimentally, however, it turned out that [41]

$$S_G = 0.240 \pm 0.016 , \tag{5.10}$$

or equivalently $\int dx(\bar{u}-\bar{d}) = -0.140 \pm 0.024$, which means an excess of $d\bar{d}$ sea quark pairs over $u\bar{u}$ ones in the physical proton state. This is a striking conclusion, considering that most of the previous parton model analyses have been performed under the assumption of isospin symmetric sea. It has been suggested by several authors that this isospin asymmetric sea is due to the pionic contribution to the sea quark distribution [43–46]. The idea of Henley and Miller is especially simple [43]. According to them, the $q\bar{q}$ pairs in the nucleon are created through the virtual dissociation processes of the valence (u and d) quarks as follows:

$$u \to \pi^+ + d , \quad u \to \pi^0 + u , \tag{5.11}$$

$$d \to \pi^- + u , \quad d \to \pi^0 + d . \tag{5.12}$$

Taking account of the quark content of the pion as

$$\pi^+ \sim u\bar{d} , \tag{5.13}$$

$$\pi^0 \sim \frac{1}{\sqrt{2}}(u\bar{u} - d\bar{d}) , \tag{5.14}$$

$$\pi^- \sim d\bar{u} , \tag{5.15}$$

one immediately notices that the emission of π^0 creates the same numbers of the $u\bar{u}$ and $d\bar{d}$ pairs and consequently does not contribute to S_G. On the other hand, $u \to \pi^+ + d$ and $d \to \pi^- + u$ generate the difference between the numbers of $u\bar{u}$ and $d\bar{d}$ pairs. By this reasoning, Henley and Miller concluded that the pionic contribution to the difference between the number of $d\bar{d}$ pairs and $u\bar{u}$ ones in the proton is equal to the difference between the number of π^+ and π^- in the proton. This is a quite probable explanation, but the problem lies in the difficulty of getting a reliable estimate of the pion numbers in the physical nucleon state. As a consequence, there also exist many other explanations of the NMC result. For instance, some authors have tried to explain the NMC data as nuclear effects, i.e., the meson exchanges and binding effects etc. [47,48]. (Remember that the NMC measurement uses the deuteron target instead of the neutron.) Other author suspects the isospin invariance itself [49]. That is, the possibility that the quark distribution functions of the proton and the neutron are not related by the isospin transformation has been discussed. It is certainly true that all these possibilities must be examined very carefully before getting a decisive conclusion [50–52]. Nonetheless, an important message from the Henley-Miller analysis is that there is an apparent asymmetry in the numbers of u and d valence quarks in the nucleon, and because of this asymmetry, there is no *a priori* reason to believe that the $q\bar{q}$ sea in the nucleon is isospin symmetric, even though the isospin symmetry itself holds exact.

Now combining the above discussion with the analysis in the preceding sections, it is quite obvious that the chiral quark soliton model is such a model that takes account of the physics of the Gottfried sum just enough in the sense that it automatically simulates the effect of pion cloud [12,13]. A key problem here is how to relate such high-energy measurements to predictions of low-energy models as studied here. Although the quark distribution functions themselves cannot be calculated reliably within the framework of low-energy models, some of their linear combinations integrated over x variable may be related to low-energy matrix elements at least approximately. As for the Gottfried sum, a plausible candidate deduced from Eq. (5.4) is the proton matrix element

$$S_G = \tfrac{1}{3}\langle p|\hat{O}|p\rangle \tag{5.16}$$

of the operator $\hat{O}$ given as

$$\hat{O} = \int d^3x \left[\left[\psi_+^\dagger(x) \frac{1+\tau_3}{2} \psi_+(x) - \psi_-^\dagger(x) \frac{1+\tau_3}{2} \psi_-(x) \right] - \left[\psi_+^\dagger(x) \frac{1-\tau_3}{2} \psi_+(x) - \psi_-^\dagger(x) \frac{1-\tau_3}{2} \psi_-(x) \right] \right]$$
$$= \int d^3x [\psi_+^\dagger(x)\tau_3\psi_+(x) - \psi_-^\dagger(x)\tau_3\psi_-(x)] . \tag{5.17}$$

[The variable x here denotes the spatial coordinate and should not be confused with the Feynman variable appearing in Eq. (5.1) etc.] Here ψ_+ and ψ_- are, respectively, the positive- and negative-frequency parts of the quark field operator ψ. (This peculiar expression appears since $\int_0^1 dx[u(x)-\bar{u}(x)]$ etc. are conserved but $\int_0^1 dx[u(x)+\bar{u}(x)]$ etc. are not.) Unfortunately, this decomposition is somewhat ambiguous. This ambiguity originates from the fact that there is no rigorous correspondence between the valence- and sea-quark concept in the present model and the corresponding idea in the standard quark parton model. Two simple possibilities have been studied here The first (most reasonable) decomposition is based on the expansion of the field operator ψ in terms of the eigenfunctions of the free (vacuum) Hamiltonian H_0. As an alternative second choice, we also investigate the decomposition of ψ in terms of the eigenfunctions of the static Hamiltonian H with the (self-consistent) background potential $U(x)$. These two lead to different decomposition of ψ into ψ_+ and ψ_-, although their sum is unique. We expect that the first choice rather than the second matches the quark-parton model interpretation of the Gottfried sum. (Incidentally, we found that the numerical difference between these two alternatives is fairly small for S_G. See the discussion below.)

It is convenient to introduce projection operators $P_\pm$ (with the property $P_+ + P_- = 1$) defined by $\psi_\pm = P_\pm \psi$. For the first choice, it is expressed as

$$P_+ = \sum_{\epsilon_i > 0} |k_i\rangle\langle k_i| , \quad P_- = \sum_{\epsilon_i < 0} |k_i\rangle\langle k_i| , \tag{5.18}$$

where $|k_i\rangle$ are the eigenstates of the free hamiltonian H_0

with the eigenenergies ϵ_i, i.e., $H_0|k_i\rangle=\epsilon_i|k_i\rangle$. [They are the plane-wave states and the sums in Eqs. (5.18) should be actually replaced by integrals.] With the quantities defined so far, the operator $\hat{O}$ is expressed as

$$\hat{O}=\int d^3x\ \psi^\dagger(x)(\tau_3-\{\tau_3,P_-\}_+)\psi(x)\ . \tag{5.19}$$

Now we are ready to use general formulas given in Sec. II for evaluating the nucleon matrix elements of arbitrary quark bilinear operators. The first nonvanishing contribution to the Gottfried sum comes from the first-order term in the collective angular velocity. The answer is given in the form

$$S_G=\tfrac{1}{3}(1-\delta_G)\ , \tag{5.20}$$

where

$$\delta_G=\delta_{\rm val}+\delta_{\rm VP} \tag{5.21}$$

with

$$\delta_{\rm val}=\frac{1}{I}\frac{N_c}{2}\sum_{m\neq 0}\frac{\langle 0|\tau_3|m\rangle\langle m|\{\tau_3,P_-\}_+|0\rangle}{E_m-E_0}\ , \tag{5.22}$$

$$\delta_{\rm vp}=\frac{1}{I}\frac{N_c}{8}\sum_{m,n}f(E_m,E_n;\Lambda)\langle n|\tau_3|m\rangle\langle m|\{\tau_3,P_-\}_+|n\rangle\ . \tag{5.23}$$

A slight complication as compared to the case of the isospin expectation value arises through the appearance of the projection operator P_-. This however causes no essential difficulty, since we know all the single-quark wave functions which are numerically given as linear combinations of the (discretized) plane-wave basis $|k_i\rangle$ [8,26].

To get some feeling about the size of the uncertainties resulting from the ambiguity of the decomposition $\psi=\psi_+ +\psi_-$, let us also investigate the second choice. This amounts to taking

$$P_+=\sum_{m>0}|m\rangle\langle m|\ ,\quad P_-=\sum_{m<0}|m\rangle\langle m|\ . \tag{5.24}$$

Here $|m\rangle$ is the eigenstates of the static Hamiltonian H, with $\sum_{m>0}$ and $\sum_{m<0}$, respectively, stand for the summation over the positive- and negative-energy eigenstates. In this case, the theoretical expression for S_G reduces to

$$S_G'=\frac{1}{3}\left[1-\frac{1}{I}(I_{\rm val}^{<}+2I_{\rm VP}^{<})\right]\ , \tag{5.25}$$

where

$$I_{\rm val}^{<}=\frac{N_c}{2}\sum_{m<0}\frac{\langle 0|\tau_3|m\rangle\langle m|\tau_3|0\rangle}{E_m-E_0}\ , \tag{5.26}$$

$$I_{\rm VP}^{<}=\frac{N_c}{8}\sum_{m,n(n<0)}f(E_m,E_n;\Lambda)\langle n|\tau_3|m\rangle\langle m|\tau_3|n\rangle\ . \tag{5.27}$$

Here we have attached prime on S_G, to distinguish it from the Gottfried sum obtained from more reasonable first choice. Numerically, we find that $I_{\rm val}^{<}\simeq 0$ and $I_{\rm VP}^{<}\simeq I_{\rm VP}/2$, so that

$$S_G'\simeq\frac{1}{3}\left[1-\frac{I_{\rm VP}}{I}\right]\ . \tag{5.28}$$

On the other hand, based on an intuititve reasoning within a similar model, Stern and Clement claimed that S_G is related to the isospin fraction of the proton carried by the pion fields as [46]

$$S_G=\frac{1}{3}\{1-\langle\tau_3\rangle_\pi\}=\frac{1}{3}\left\{1-\frac{I_\pi}{I}\right\}\ , \tag{5.29}$$

where I_π represents the pionic contribution to the moment of inertia. By identifying $I_{\rm VP}/I$ with I_π/I, our argument leading to Eq. (5.28) then roughly justifies the above simple formula given by Stern and Clement [46]. We however emphasize that S_G in Eq. (5.20) is more realistic than S_G' above. Anyhow, in the light of our derivation here, we clearly see that there is no rigorous justification of their simple formula. The same is also true for the Henley-Miller assertion that the Gottfried sum measures the difference between the numbers of π^+ and π^- in the nucleon [43].

Shown in Table VII are the theoretical predictions for the Gottfried sum S_G together with the parameter δ_G defined in Eqs. (5.21) and (5.23). The vacuum polarization contribution to the isovector charge (or the isospin fraction carried by the sea quarks) and S_G' evaluated with the formula (5.25) are also shown for reference. One certainly confirms that the values of S_G' are not extremely different from those of S_G especially for not so large values of M. For the quantity δ_G, only the total contribution is shown, since the decomposition into $\delta_{\rm val}$ and $\delta_{\rm VP}$ has no particular physical meaning. (We only comment that $\delta_{\rm val}$ term gives almost negligible contribution as compared to the $\delta_{\rm VP}$ term.) One might notice that the magnitudes of $\langle\tau_3\rangle_{\rm VP}=I_{\rm VP}/I$ and δ_G are comparable to each other, although the difference becomes a little larger as M increases. By definition, the quantity δ_G parametrizes the deviation of S_G from 1/3. Putting all of these together, we then conclude that the observed deviation of S_G from 1/3 can be attributed to isospin-nonsinglet excitation of $q\bar{q}$ pairs. In other words, $q\bar{q}$ sea is likely to carry a sizable fraction of the nucleon isospin. Since this $q\bar{q}$ excitation is roughly identified with the pion cloud surrounding the core of N_c valence quarks, our analysis of the NMC experiment gives a strong support to that of Henley and Miller and others [43–46].

TABLE VII. The isospin contents, the parameter δ_G defined in Eq. (5.21), and the Gottfried sum S_G, given as functions of M. The numbers in the parentheses of the fifth column of the table corresponds to S_G' in Eq. (5.25).

M (MeV)	$I_{\rm val}/I$	$I_{\rm VP}/I$	δ_G	S_G	(S_G')
350	0.870	0.130	0.136	0.288	(0.291)
375	0.824	0.176	0.189	0.270	(0.277)
400	0.789	0.211	0.230	0.257	(0.265)
425	0.759	0.241	0.265	0.245	(0.256)
450	0.733	0.267	0.296	0.235	(0.247)

To sum up, the isospin asymmetry of the $q\bar{q}$ sea in the nucleon is most likely to exist as a combined effect of the spontaneous chiral-symmetry breaking and the asymmetry of the u and d valence quark numbers in the nucleon.

VI. CONCLUDING REMARKS

According to Shuryak again [1], a new general trend of hadron physics is to understand the properties of the QCD vacuum rather than to just explain the properties of hadrons such as their masses and magnetic moments. He also emphasizes that the understanding of the role of the light quarks (u,d,s) is a key ingredient in the phenomenology of the QCD vacuum. As is widely believed, the QCD vacuum is characterized by the nonvanishing quark condensate which signals the spontaneous breaking of the chiral symmetry possessed by the original Lagrangian. (The gluon condensate is not considered here, since the gluonic degrees of freedom is treated only implicitly in the present analysis.) Although there still remain some questions as to how this fundamental property of the QCD vacuum is realized, there is no doubt that this phenomena would not be expected without the Dirac-sea-quark degrees of freedom. This in turn means that, if we attempt to understand the properties of baryons simultaneously with that of the QCD vacuum, we must necessarily deal with the valence and sea quarks on equal footing. At first sight, it seems to be a formidable task, but it in fact turned out feasible on the basis of the chiral quark soliton model.

The most instructive example for understanding the above statement may be provided by our analysis of the spatial dependence of the isoscalar scalar condensate inside the nucleon. This analysis most clearly shows that the nontrivial local structure of the quark condensate arises from an interplay of the valence- and sea-quark degrees of freedom. This local defect in the nonperturbative QCD vacuum (with the homogeneous quark condensate) is far from an "empty" bubble containing three valence quarks as suggested by the original version of the MIT bag model. Instead, the valence quarks contained in it turns out to be surrounded by the $q\bar{q}$ excitation or the cloud of pions. This interesting spatial structure of the quark condensate is however not directly measurable. In order to connect the prediction of the model with some observables, we have analyzed the spatial integrals of the scalar condensates, especially their isospin structure. We found that the isoscalar dominance of the $\bar{q}q$ scalar condensate relative to the isovector one (or the enhancement of $\bar{d}d$ scalar condensate relative to the $\bar{u}u$ one in the proton) predicted by the theory is consistent with the low-energy QCD phenomenology. It was also shown that the chiral quark soliton model naturally explains the characteristic feature of the neutron charge distribution, by automatically simulating the effect of the negatively charged pion cloud at long distances. In this neutron charge density problem, it is almost self-evident where the isospin asymmetry of the pion cloud (or equivalently that of the $\bar{q}q$ excitation) comes from. The obvious asymmetry existing in the valence quarks numbers inside the nucleon is the eventual cause of the above asymmetry. From this consideration, the flavor asymmetry of the $q\bar{q}$ sea suggested by the recent NMC experiment seems nothing surprising but only natural. In fact, the size of the asymmetry of the $\bar{q}q$ sea extracted from this experiment turns out to be order of magnitude consistent with the prediction of the chiral quark soliton model with the reasonable range of the model parameter M.

To summarize, the degrees of freedom of the Dirac-sea quarks are not only essential for generating nonvanishing vacuum quark condensate but also important for creating the flavor- (isospin-) asymmetric pionic excitation inside the nucleon through the mutual interaction with the valence quarks contained in it. The resultant nucleon picture appears to be completely consistent with the recent NMC measurement of the Gottfried sum. Throughout the paper, we have neglected the strange quark degrees of freedom under the assumption that the $s\bar{s}$ components in the nucleon is very small [53]. However, the essential features of our findings in the present study would not be altered, even if this assumption is a little modified.

ACKNOWLEDGMENTS

The author would like to express his sincere thanks to Professor S. Platchkov for sending the numerical data of their analysis of the neutron electric form factor. The numerical calculation was performed by using the FACOM M-1800/20 computer at the Research Center for Nuclear Physics, and the NEAC ACOS 2000 Computer at the Computer Center, Osaka University, financially supported in part by the Research Center for Nuclear Physics, Osaka University. This work was supported by the Grant-in-Aid of Scientific Research, Ministry of Education, Science and Culture, Japan.

[1] E. V. Shuryak, *The QCD Vacuum, Hadrons and the Superdense Matter* (World Scientific, Singapore, 1988), Chap. 8.
[2] D. I Diakonov and V. Yu. Petrov, Nucl. Phys. **B272**, 457 (1986).
[3] D. I. Diakonov, V. Yu. Petrov, and P. V. Pobylitsa, Nucl. Phys. **B306**, 809 (1988).
[4] H. Reinhardt and R. Wünsch, Phys. Lett. B **215**, 577 (1988).
[5] H. Reinhardt and R. Wünsch, Phys. Lett. B **230**, 93 (1989).
[6] Th. Meissner, E. Ruiz Arriola, F. Grümmer, H. Mavromatis, and K. Goeke, Phys. Lett. B **214**, 312 (1988).
[7] Th. Meissner, F. Grümmer, and K. Goeke, Phys. Lett. B **227**, 296 (1989).
[8] M. Wakamatsu and H. Yoshiki, Nucl. Phys. **A524**, 561 (1991).
[9] I. Adjali, I. J. R. Aitchison, and J. A. Zuk, Nucl. Phys. **A537**, 457 (1992).
[10] M. Wakamatsu (unpublished).
[11] S. Forte, Phys. Lett. B **224**, 189 (1989); Nucl. Phys. **B331**,

1 (1990).
[12] M. Wakamatsu, Phys. Rev. D **44**, 2631 (1991).
[13] M. Wakamatsu, Phys. Lett. B **269**, 394 (1991).
[14] J. A. Zuk, Z. Phys. C **29**, 303 (1985).
[15] I. J. R. Aitchison and C. M. Fraser, Phys. Rev. D **31**, 2605 (1985).
[16] A. Dhar, R. Shankar, and S. R. Wadia, Phys. Rev. D **31**, 3256 (1985).
[17] D. Ebert and H. Reinhardt, Nucl. Phys **B271**, 188 (1986).
[18] P. Simic, Phys. Rev. D **34**, 1903 (1986).
[19] M. Wakamatsu and W. Weise, Z. Phys. A **331**, 173 (1988); M. Wakamatsu, Ann. Phys. (N.Y.) **193**, 287 (1989).
[20] J. Gasser and H. Leutwyler, Phys. Rep. **87**, 77 (1982).
[21] M. Gell-Mann, R. J. Oakes, and B. Renner, Phys. Rev. **175**, 2195 (1968).
[22] D. I. Diakonov, V. Yu. Petrov, and M. Praszalowicz, Nucl. Phys. **B323**, 53 (1989).
[23] P. J. Mulders, Phys. Rev. D **30**, 1073 (1984).
[24] I. Zahed, A. Wirzba, and U.-G. Meissner, Ann. Phys. (N.Y.) **165**, 406 (1985).
[25] S. Kahana, G. Ripka, and V. Soni, Nucl. Phys. **A415**, 351 (1984).
[26] S. Kahana and G. Ripka, Nucl. Phys. **A429**, 462 (1984).
[27] T. H. R. Skyrme, Proc. R. Soc. London **A260**, 127 (1961).
[28] G. S. Adkins, C. R. Nappi, and E. Witten, Nucl. Phys. **B228**, 552 (1983).
[29] H. Reinhardt, Nucl. Phys. **A503**, 825 (1989).
[30] K. Goeke, A. Z. Górski, F. Grümmer, Th. Meissner, H. Reinhardt, and R. Wünsch, Phys. Lett. B **256**, 321 (1991).
[31] A. J. Niemi and G. W. Semenoff, Phys. Rep. **135**, 99 (1986).
[32] A. J. Niemi, in *High Energy Physics,* edited by M. J. Bowick and F. Gürsey (World Scientific, Singapore, 1986), Vol. 1, p. 125.
[33] G. E. Brown, M. Rho, and W. Weise, Nucl. Phys. **A454**, 669 (1986).
[34] U.-G. Meissner, N. Kaiser, and W. Weise, Nucl. Phys. **A466**, 685 (1987).
[35] T. Watabe and H. Toki, Prog. Theor. Phys. **87**, 651 (1992).
[36] A. Jackson, A. D. Jackson, and V. Pasquier, Nucl. Phys. **A432**, 567 (1985).
[37] H. Yabu and K. Ando, Prog. Theor. Phys. **74**, 750 (1985).
[38] M. Gari and W. Krümpelmann, Z. Phys. A **322**, 689 (1985).
[39] S. Platchkov *et al.*, Nucl. Phys. **A510**, 740 (1990).
[40] R. D. Peccei, in *Concepts and Trends in Particle Physics,* edited by H. Latal and H. Mitter (Springer, Berlin, 1987), p. 223.
[41] NMC Collaboration, P. Amaudruz *et al.*, Phys. Rev. Lett. **66**, 2712 (1991).
[42] F. E. Close, *An Introduction to Quarks and Partons* (Academic, London, 1979), Chap. 13.
[43] E. M. Henley and G. A. Miller, Phys. Lett. B **251**, 453 (1990).
[44] S. Kumano, Phys. Rev. D **43**, 59 (1991).
[45] S. Kumano and J. T. Londergan, Phys. Rev. D **44**, 717 (1991).
[46] J. Stern and G. Clément, Phys. Lett. B **264**, 426 (1991).
[47] L. P. Kaptari and A. Yu. Umnikov, Phys. Lett. B **272**, 359 (1991).
[48] L. N. Epele, H. Franchiotti, C. A. García Canal, and R. Sassot, Phys. Lett. B **275**, 155 (1992).
[49] B.-Q. Ma, Phys. Lett. B **274**, 111 (1992).
[50] G. Preparata, P. G. Ratcliffe, and J. Soffer, Phys. Rev. Lett. **66**, 687 (1991).
[51] S. D. Ellis and W. J. Stirling, Phys. Lett. B **256**, 258 (1991).
[52] E. Sather, Phys. Lett. B **274**, 433 (1992).
[53] R. L. Jaffe and C. L. Korpa, Comments Nucl. Part. Phys. **17**, 163 (1987).